Design considerations for ferrofluid pressure bearing pads

van den Toorn, Stefan W.M.; Spronck, Jo W.; van Ostayen, Ron A.J.; Lampaert, Stefan G.E.

DOI
10.1016/j.rineng.2021.100200

Publication date
2021

Document Version
Final published version

Published in
Results in Engineering

Citation (APA)
van den Toorn, S. W. M., Spronck, J. W., van Ostayen, R. A. J., & Lampaert, S. G. E. (2021). Design considerations for ferrofluid pressure bearing pads. *Results in Engineering*, *10*, Article 100200. https://doi.org/10.1016/j.rineng.2021.100200

Results in Engineering 10 (2021) 100200

Contents lists available at ScienceDirect

Results in Engineering

journal homepage: www.editorialmanager.com/rineng/Default.aspx

Design considerations for ferrofluid pressure bearing pads

Stefan W.M. van den Toorn *, Jo W. Spronck, Ron A.J. van Ostayen, Stefan G.E. Lampaert

Department of Precision and Microsystems Engineering, Delft University of Technology, Delft, the Netherlands

ARTICLE INFO

Keywords:
Magnetic fluid
Air bearing alternative
Aerostatic alternative
Stick-slip
Wear free
Planar positioning
Precise positioning

ABSTRACT

The novel contribution of this research is insight into the influence of different parameters in the magnet configurations on the load and stiffness of a ferrofluid pressure bearing. It is shown that magnets with a small cross-section magnetized alternatively up and downwards combine a high load capacity and moderate stiffness while being low on material cost and complexity. The configuration where magnets are placed alternatively in left and right direction magnetized inter spaced with iron yields the highest load capacity and stiffness, albeit at the cost of weight and complexity. It is shown that an increase in the number of magnets is beneficial for the stiffness in both magnetization configurations, as is an increase in remanent flux density of the magnet. A metal bottom plate made of iron reduces the necessary height of the magnet in the up-down magnetization configuration. The model was validated using a bearing pad arranged in the up-down configuration. The force-displacement curve of this pad was measured in a load frame, using the APG 513 A ferrofluid from Ferrotec. A load capacity of 1.75 N/cm^2 was achieved, this exceeds previous pressure bearing implementations and performs comparable or better than implementations of single seal ferrofluid pocket bearings. These results show that the ferrofluid pressure bearing is a passive alternative in motion systems where the designer otherwise would have needed to use an active bearing.

1. Introduction

Plain bearings have many benefits, such as compact design, easy of manufacturing, high resistance to shocks, low vibration levels, and low levels of fatigue [1]. However, they are not generally found in precise motion systems as they suffer from stick-slip effects. This prevents a smooth continuous motion of the bearing, especially at low speeds [2]. The bearings that are commonly found in precise motion systems are expensive, have a need for active components or are complex [3]. The ferrofluid bearing has none of these issues while still having all the benefits of the plain bearing [4]. A major difference between the plain and ferrofluid bearing is that the ferrofluid bearing doesn't exhibit stick slip effects. Because of this the ferrofluid bearing is an excellent alternative to the bearings commonly used in precise motion systems.

The ferrofluid bearing consists out of a magnet array and a magnetic fluid. This fluid is a colloidal suspension consisting of magnetic particles in a carrier fluid [5]. In a magnetic field these particles are drawn to the highest field intensity and as a result produce a pressure in the fluid. A bearing can be created by placing the fluid in a magnetic field in between two bearing surfaces [6]. As the bearing is loaded, the surfaces move closer together and the fluid is displaced from the equilibrium position, which in turn induces a reaction force. This is called the ferrofluid pressure bearing. Alternatively, the pressure in the fluid can be used to seal a pocket of air and a displacement of the bearing surface will pressurize this air resulting in a normal force. This is called the pocket bearing [4].

Fig. 1 shows the working principle of the ferrofluid pressure bearing. Using equations (1) and (2) the load and stiffness of the pressure bearing can be calculated [7]. In these equations F_L is the load capacity, μ_0 the permeability in vacuum, M_s the saturation magnetization of the ferrofluid and H the magnetic field intensity. The area is defined as the surface area of the ferrofluid on the top bearing surface. It can be seen in Fig. 1 that an increase in payload causes the bearing surfaces to move closer together, thus increasing the area over which the integral is taken, as well as increasing the overall magnetic field intensity. In practice only the former effect will be significant as the outer fluid edge is already at a low, and close to constant, magnetic field intensity.

$$F_L = \mu_0 M_s \int_S H dA \tag{1}$$

* Corresponding author.
E-mail address: stefanvandent@gmail.com (S.W.M. van den Toorn).

https://doi.org/10.1016/j.rineng.2021.100200
Received 13 February 2020; Received in revised form 30 December 2020; Accepted 7 January 2021

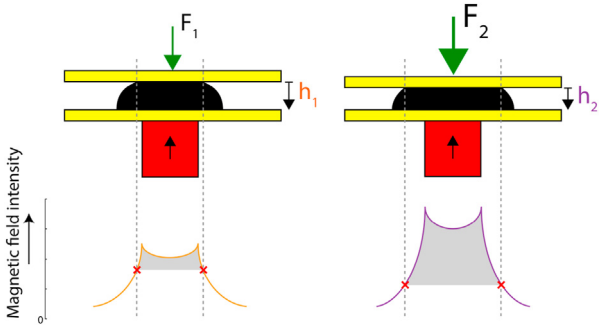

Fig. 1. Effect of increase in payload in a ferrofluid pressure bearing with magnetic field intensity at the location of the top bearing surface. With $F_1 < F_2$ and $h_1 > h_2$.

$$k = -\mu_0 M_s \frac{d}{dh} \int_S HdA \tag{2}$$

While ferrofluid bearings exist in literature [8–11], the implementation suffers from repeatability issues and/or lack in load capacity and stiffness. This lack of repeatability in these studies is mainly the result of the use of the ferrofluid pocket bearing [4], due to the fact that air will escape from the pocket when overloaded. The repeatability of the pressure bearing is in principal much higher as no air can escape. However, the currently designed ferrofluid pressure bearings exhibit a limited load capacity and low stiffness. The optimal configuration of pocket bearings has already been determined by Boots [12], however, this has yet to be done for the pressure bearing.

The optimal pressure bearing consists of an optimal fluid in an optimal magnetic field. Research has been done on the magnetic fluid. Although not specifically for bearing applications, there are some fluids that are well suited. Less is known about the design of the optimal magnetic field. Thus, this research will focus on the design of the magnetic field for high load capacity and stiffness and the impact on material cost and complexity. The novelty of the work in this research is the insight in the design of the magnetic field for the application in a pressure bearing pad and the direct comparison between the pressure and pocket bearing.

2. Modelling of pressure bearing pad

The magnetic field can be manipulated by arranging multiple magnets in relation to each other with the addition of metal with high permeability. In order to obtain an understanding of the influence of the different parameters, a model has been made.

The pressure bearing model is based on a 2D simulation of a cross-section of the bearing pad using the AC/DC module in COMSOL Multiphysics [13]. This simulation assumes the bearing pad to continue infinitely in and out of the plane as seen in Fig. 2. The error in simulation caused by the finite bearing length is evaluated in a 3D model and found to be negligible. Using the LiveLink interface, a COMSOL model is parametrically coded in Matlab [14], solved in COMSOL and then post-processed in Matlab. Fillets were applied to all corners in order to prevent singularities from occurring. Iron is modelled using the B–H curve for soft iron (with losses) material in the built in COMSOL library, magnets are modelled with a uniform remanent flux density, and the air and ferrofluid are modelled as having a relative permeability equal to one.

In this model several design parameters were varied, these are listed in Fig. 2 and Table 1. The Halbach magnetization configuration was left out as it produces a constant field with little gradient, which would result in a low stiffness bearing [15]. The build volume was taken to be 50 × 100 × 4 mm (width x length x height), the length being defined perpendicular to the plane as seen in Fig. 2. The constants used in modelling the pressure bearings can be seen in Table 2 and Fig. 2. As the minimum fly height is dictated by manufacturing tolerances and damping, it is set at 0.1 mm for all parameter configurations. For the metal between the magnets and for the bottom plate iron has been chosen for its high permeability and saturation magnetization. The gaps are modelled as air.

The load capacity and stiffness of the different configurations are found using equation (1). For the load capacity the surface integral of the magnetic field is determined at a fly height of 0.1 mm. The stiffness is determined by evaluation of the load capacity increase from a fly height equal to 0.1 mm to a fly height equal to 0.095 mm.

The width of the metal and magnets is defined using the parameters and can be found using equations (3) and (4) respectively. The definition of the symbols used can be seen in Table 1.

$$W_{mag} = \left(Width - W_{gap}\left(N_{mag} - 1\right)\right) \frac{1 - R_{\frac{Met}{Mag}}}{N_{mag}} \tag{3}$$

Table 1
Design parameters and their respective ranges.

Variable	Symbol	Type	Range	Unit	Range based on
Number of magnets	N_{mag}	Discrete	1–50	–	Manufacturability
Magnetization direction of magnets	Mag_{dir}	Discrete	↑↓, ↑↑, ↑←, ←→,	–	Assumed optimum
Width of gap	W_{gap}	Continuous	0–3	mm	Assumed optimum
Ratio metal to magnet	$R_{\frac{Met}{Mag}}$	Continuous	0–0.5	–	Assumed optimum
Thickness metal bottom plate (MBP)	H_{mbp}	Continuous	0–2	mm	Assumed optimum
Height of magnet	H_{mag}	Continuous	0.5–4	mm	Manufacturability
Remanent flux density of the magnet	Mag_{str}	Continuous	1.1–1.5	T	Manufacturability

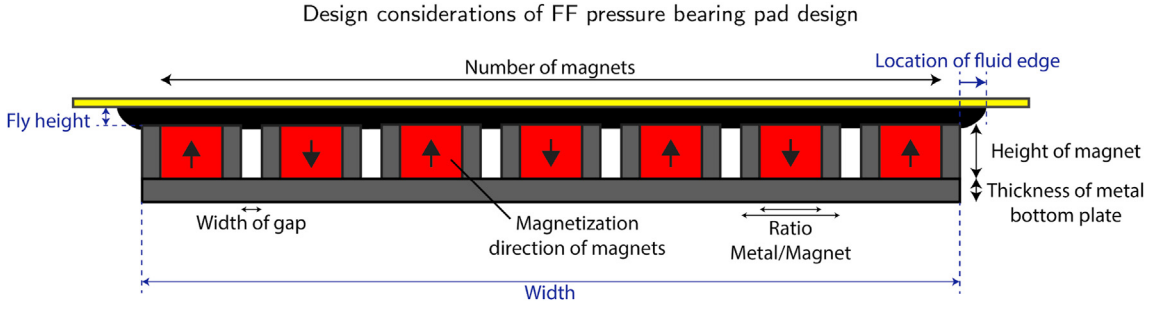

Fig. 2. Design parameters (black) and model constants (blue) in a cross-section of the bearing pad. The length of the pad is defined into the plane. (For interpretation of the references to colour in this figure legend, the reader is referred to the Web version of this article.)

Table 2
Model constants.

Constant	Value	Unit
Width	50	mm
Length	100	mm
Fly height	0.1	mm
Relative permeability ferrofluid	1	–
Saturation magnetization ferrofluid	52.5	kA/m
Relative permeability metal	4000	–
Saturation magnetization metal	1.4	T
Relative permeability magnets	1	–
Location fluid edge	5	mm

$$W_{met} = \frac{1}{2} R_{\frac{Met}{Mag}} W_{mag} \tag{4}$$

2.1. Initial optimization

Initially, a parameter sweep is performed using several evaluation points in the range of each parameter. From this initial parameter sweep it could be concluded that the magnetization direction of the magnets has a great influence on the design of the bearing pad. The results of the parameter sweep were subsequently used in an optimization for stiffness. Constraints were added using a penalty method. The imposed constraints were a minimum load capacity of 100 N, a maximum weight of 150 g and a maximum material cost of €50. These constraints are based on a particular linear stage design with a mover supported on pressure bearing pads. Equation (5) relates the cost of the magnetic material per gram (Y) as a function of the remanent flux density of the magnet (M_{str}). This equation was based on data retrieved from the online design tool of HKCM [16]. Using this tool, the cost of a large magnet with different remanent flux densities was calculated. From this data the function was determined using the Matlab curve fitting toolbox. It must be noted that this is a rough estimate and it can only be used as a relative measure of cost of the different magnet configurations. The material cost of metal was assumed to be negligible.

$$Y = \left(2.4 \cdot 10^{-3}\right) e^{3.7293 \cdot M_{str}} \tag{5}$$

Table 3 shows the results of the parameter sweep for different magnet magnetization directions. Some interesting observations are:

Table 3
Optimized magnet configuration for stiffness subjected to constraints: load capacity > 100 N, cost < €50, weight <150 g. Using the constants in Table 2. Fly height for all configurations is 0.1 mm.

Variable	Values	Unit				
Magnetization direction of magnets	↑↓, ↑↑, ↑←, ←→	–	Up-Down	Up-Up	Up-Left	Left-Right
Number of magnets	5, 15, 30, 40, 50	–	50	30	30	50
Remanent flux density of the magnet	1, 1.15, 1.3, 1.5	T	1.5	1.5	1.5	1.5
Height of magnet	1, 2, 3	mm	1	1	2	3
Ratio metal to magnet	0, 0.2, 0.4	–	0	0.4	0.2	0.4
Thickness metal bottom plate	0, 1	mm	1	1	0	0
Width of gap	0, 0.1, 0.2	mm	0	0	0.2	0
Material cost		€	24.19	17.28	35.64	51.83
Weight		g	77.5	78.2	67.0	114.6
Load capacity		N	149.63	117.09	128.22	216.46
Stiffness		N/μm	0.52	0.52	0.68	0.76

- All magnetization directions use the highest remanent flux density for the magnet that is available.
- A gap in between magnets is unwanted in all magnetization directions except up-left, this is a result of a slight increase in stiffness as the gap increases.
- The up-down magnetization array is relatively simple compared to the others, no additional ferromagnetic material or gaps are used.
- The left-right magnetization direction shows the best performance. This however comes at the cost of complexity as small features are required. Much material is required relative to the other magnetization directions, resulting in a higher weight.

From the initial parameter sweep it can thus be concluded that each magnetization direction produces a different optimal configuration of magnets, metal and gaps. The choice of magnetization direction is based on the trade-off between weight, material cost, load capacity, stiffness and complexity. The up-down magnetization configuration is preferred for the relatively low material cost and complexity while still having a moderate load capacity. The combination of low material cost and low complexity can result in a very cheap to produce bearing design. The absence of gaps and metal makes for a potentially monolithic bearing. The magnetization can then be 'written' on a single block of Ne-Fe-B [17–19]. A single magnet block can significantly reduce assembly complexity as well as improve tolerances. The up-down and left-right magnetization configurations are both suited for bearing applications and they will be discussed next.

2.2. Up-down magnetization configuration

Fig. 3 shows the magnet configuration using the parameters in Table 3 with the magnetic field intensity at 0.1 mm. The neighbouring magnets provide a low reluctance path which results in a spike in the magnetic field intensity. Due to the large number of magnets, many low reluctance paths are created. This moves the overall magnetic field intensity closer to the magnet, increasing load capacity and stiffness.

Table 4 shows the effect of the different parameters on the stiffness normalized using logarithmic sensitivity. The sensitivities are determined around the up-down configuration in Table 3. As the gap and the ratio metal to magnet are already minimal, only the number of magnets, height of magnets, remanent flux density and fly height can improve the stiffness of the bearing. Use of a metal bottom plate has no significant effect on the bearing performance but does add moving mass if the bearing pads are mounted on the mover. An increase in the number of magnets also decreases the load capacity. Thus, a compromise has to be made.

Fig. 4 and Fig. 5 show the influence of the different parameters on the stiffness and load capacity. The metal bottom plate is more efficient for a lower number of magnets. A relative thin bottom plate of 0.5 mm is enough to prevent effects of saturation. Fig. 4 again stresses the importance of many small magnets. It can be seen that the optimum for load capacity lies around 20–25 magnets. The optimum for stiffness however is located outside of the graph. From Fig. 5 we see that the stiffness and the load capacity scale linearly with the remanent flux density of the magnet. The height of the magnets shows an optimum around 1 mm.

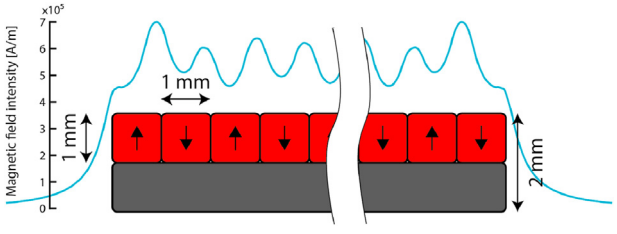

Fig. 3. Magnet configuration for up-down magnetization direction with magnetic field intensity at 0.1 mm above magnet surface.

Table 4
Logarithmic sensitivity of an increase in the individual parameters for the stiffness of the up-down magnetization configuration.

	N_{mag}	W_{gap}	H_{mag}	$R_{\frac{Met}{Mag}}$	Mag_{str}	H_{mbp}	Fly height
Stiffness	0.843	−0.002	0.113	−0.010	1	0.002	−0.282
Load capacity	−0.138	−0.001	0.105	−0.008	1	0.002	−0.280

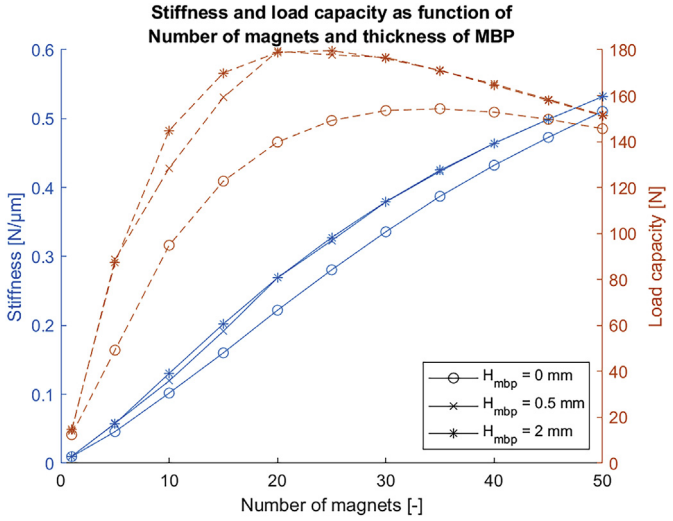

Fig. 4. Stiffness and load capacity as a function of the number of magnets for different thicknesses of the metal bottom. For up-down magnetization configuration.

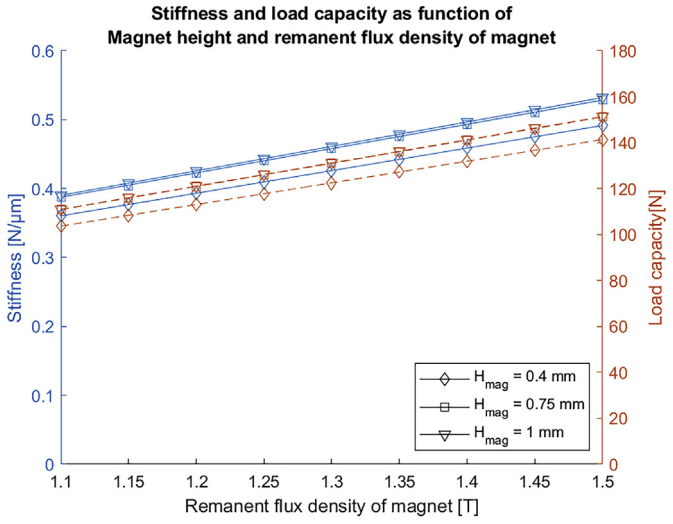

Fig. 5. Stiffness and load capacity as a function of the remanent flux density of the magnet for different heights of the magnets. For up-down magnetization configuration. The lines for magnet height of 0.75 mm and 1 mm coincide.

Further increase of the height reduces the stiffness slightly.

Fig. 6 shows the relation between the height of the magnets and the bearing performance for different thicknesses of the metal bottom plate. Up to 25% performance gain can be achieved by only 0.5 mm metal bottom plate thickness. It can be seen that in most cases it is more cost-effective to use less magnetic material and a thin metal bottom plate. Figs. 5 and 6 contain all significant parameters concerning the respective material cost and weight. It can be seen that a cost-effective bearing is to favour remanent flux density of the magnet over magnet height, while using a metal bottom plate. The same goes for optimizing towards

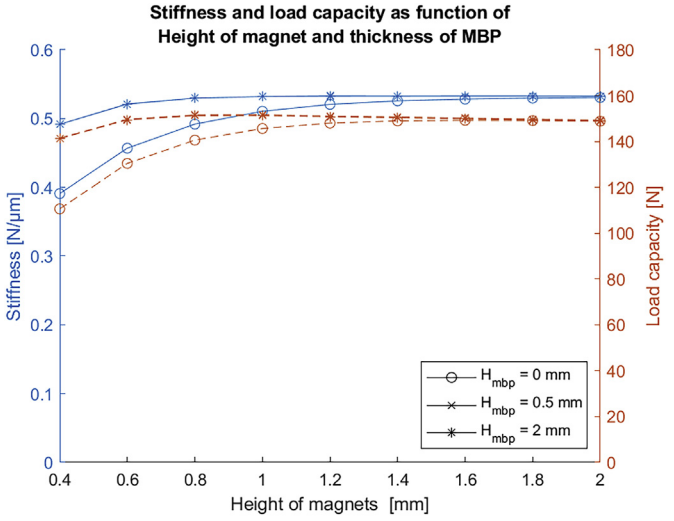

Fig. 6. Stiffness and load capacity as a function of height of magnet for different thicknesses of the metal bottom plate. For up-down magnetization configuration. The lines for 0.5 mm and 2 mm bottom plate thickness coincide.

weight, thin magnets combined with a thin metal bottom plate.

2.3. Left-right magnetization configuration

Fig. 7 shows the left-right magnetization configuration for the values of the parameters in Table 3. The study from the previous section is repeated here for the left-right magnetization configuration.

Table 5 shows the logarithmic sensitivity of the stiffness for the different parameters with the configuration in Table 3 as initial value. The width of the gap and thickness of the metal bottom plate are already zero, thus the ideal configuration doesn't include gaps or a metal bottom plate. The response of the load capacity and stiffness on change in the height of the magnet, number of magnets, metal to magnet ratio and remanent flux density of the magnet are shown in Fig. 9 and Fig. 10.

The same dependence of the number of magnets can be observed in Fig. 8 as with the up-down configuration. There is a distinct difference in the optimum of the load capacity and the stiffness. The addition of metal in between the magnets shows an increase in bearing performance. Some metal is needed to guide the magnetic field. However, this increase of the width of this metal reduces the amount of magnetic material in the

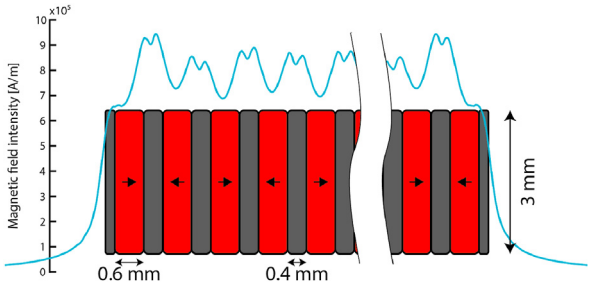

Fig. 7. Magnet configuration for left-right magnetization with magnetic field intensity at 0.1 mm above magnet surface.

Table 5
Logarithmic sensitivity of an increase in the individual parameters for the left-right magnetization configuration.

	N_{mag}	W_{gap}	H_{mag}	$R_{\frac{Met}{Mag}}$	Mag_{str}	H_{mbp}	Fly height
Stiffness	0.548	−0.012	0.343	−0.063	1	−0.006	−0.550
Load capacity	−0.590	−0.089	0.551	−0.146	1	−0.006	−0.284

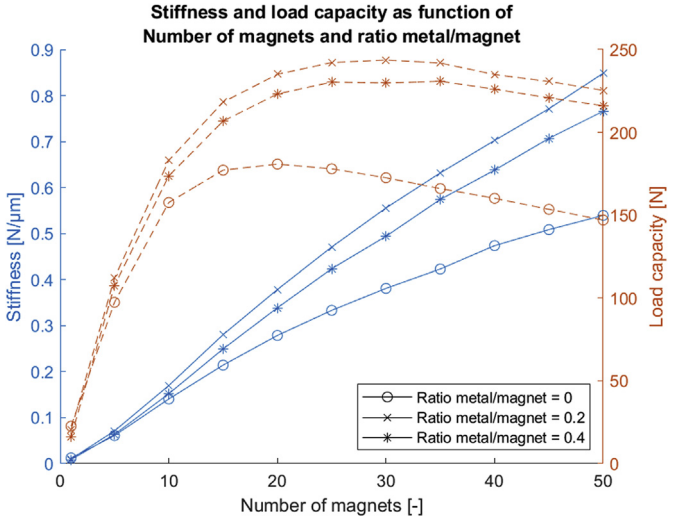

Fig. 8. Stiffness and load capacity as a function of the number of magnets for different ratios of metal to magnet. For left-right magnetization configuration.

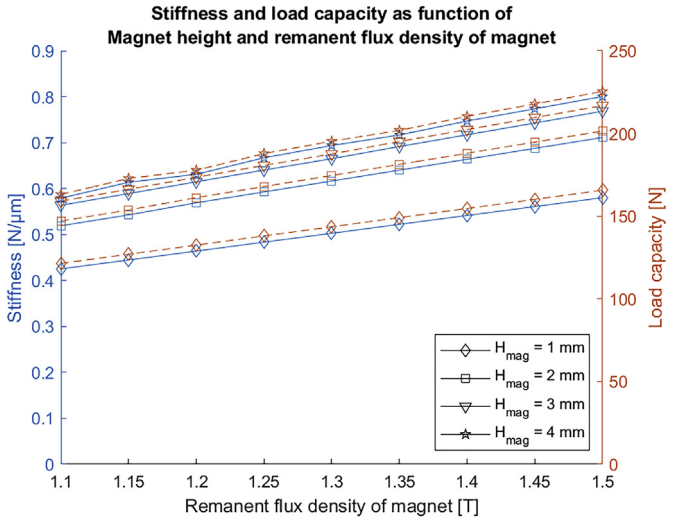

Fig. 9. Stiffness and load capacity as a function of the remanent flux density of the magnet for different heights of the magnets. For left-right magnetization configuration.

bearing configuration, thus eventually leading to a reduction of performance. Fig. 9 also shows similar behaviour for the remanent flux density of the magnet compared to the up-down configuration.

As the specific weight of neodymium magnets and metal are very similar, the weight of the configuration is determined by the height of the magnets. The material cost is determined by the remanent flux density of the magnet, height of magnets and the ratio metal to magnet.

From the influence of the specific parameters it can be concluded that the configuration using a left-right magnetization depends largely on the cost and weight constraints. As the metal bottom plate reduces the bearing performance, remanent flux will be larger using this type of

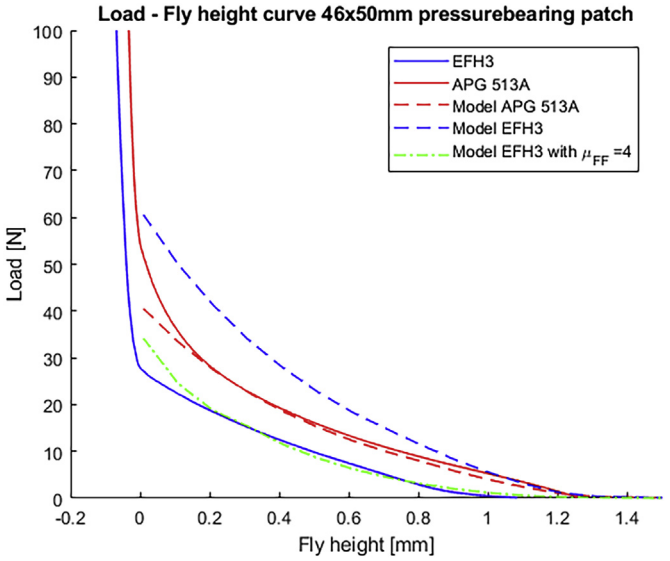

Fig. 10. Load-fly height curve of pressure bearing pad with EFH3 and APG 513 A ferrofluid and modelled performance of the ferrofluid. pad consists of 23 50×2×2mm magnets from HKCM [20] arranged in up-down configuration. The remanent flux in the magnets is 1.17 T, the location of fluid edge is modelled 0.9 mm outside magnet.

bearing. The stability will also be an issue when choosing a configuration with a small metal to magnet ratio.

3. Method for validation

A materials test frame is used to validate the model of the pressure bearing pad. This is done by a fly height sweep of a pad made up of 23 magnets with the dimensions 50×2×2mm (L×W×H) and a remanent flux density of 1.17 T [20]. The magnets are arranged in the up-down magnetization configuration. The pad is placed on a ferritic stainless-steel (AISI 410s) bottom plate and is filled with 5 g of either the EFH3 or the APG 513 A ferrofluid.

Both the APG 513 A and EFH3 fluid are manufactured by Ferrotec. The APG 513 A fluid is chosen as it is common in literature and its properties are well known [21]. The EFH3 fluid is chosen for its high magnetic saturation and low viscosity, making it a more suitable ferrofluid for use in bearings in comparison to the APG 513 A.

The load of the bearing at the same fly height sweep is modelled. The magnet dimensions, pad dimensions and remanent flux density are modelled as described above. As the location of the ferrofluid edge is found at the point where the magnetic body force acting on the fluid is overcome by the gravity force, it can be determined using a COMSOL simulation of the magnetic field surrounding the bearing pad. This location was found at 0.8 mm outside the bearing pad for the APG 513 A fluid and 0.9 mm for the EFH3 fluid. The magnetic saturation of the ferrofluids are set to 32 kA/m for the APG 513 A fluid [21] and 52.5 kA/m for the EFH3 fluid [22].

4. Results and discussion

Fig. 10 shows the results of the fly height sweep and the modelled load capacity. Zero fly height was taken to be the point at which the pressure plate touches the magnets in the measurement.

The modelling of the bearing pad using the APG 513 A fluid is in close agreement with the measurement. There is a slight divergence between the model and the measurements as the fly height approaches zero, which can be explained by the squeeze film damping from the relatively high viscous (150 mPa·s) ferrofluid.

As can be seen in formula 1, the load capacity of a bearing pad should be proportional to the saturation magnetization. This can be observed when looking at the modelled load vs fly height curve for the APG 513 A and EFH3 ferrofluid. When looking at the measurements it can be seen that while the APG 513 A measurement and model are in good agreement, the same is not true for EFH3 measurement and model.

The probable cause of this difference is the accumulation of magnetic particles in areas of high magnetic field gradients. The largest gradients in the bearing pad are located at the corners in between two magnets. Accumulation of the magnetite particles there causes effectively a short circuit of the magnetic field, reducing the magnetic field elsewhere. A relatively good approximation of the accumulation can be done by increasing the relative permeability of the ferrofluid, this can be seen in the dash-dot line in Fig. 10.

The APG 513 A fluid achieves a load capacity of 1.75e4 N/m^2. This bearing configuration exceeds previous implementations of pressure bearings [8,23,24] and performs comparable or better than implementations of single seal pocket bearings [25–27]. Still, pocket bearings can be made with an even higher load capacity by stacking seals. The downside of this bearing design is the creation of more pockets of air that all need to be managed in order to have a repeatable system behaviour.

5. Conclusion

The orientation of the different magnets in relation to each other is an important parameter in the design of pressure bearing pads. Two distinct magnetization configurations both prove promising. The up-down magnetization configuration for its simplicity, and the left-right configuration for performance.

The up-down magnetization configuration consists of an array of magnets combined with a metal bottom plate. The number of magnets is the most important parameter in this configuration, combined with the remanent flux density of the magnet. Higher amounts of magnets slightly reduce load capacity, but offer more stiffness in return. Current state of the art allows for the 'writing' of the magnetization in the magnets, this technology can allow for monolithic pressure bearings [18,19].

In the left-right magnetization configuration the magnets counteract each other, in contrast to the up-down magnetization configuration where they form low reluctance paths. This could prove problematic as the configuration can become unstable when designed with a small metal to magnet ratio. However, this configuration also potentially has higher stiffness and load capacity compared to the up-down magnetization configuration.

In the bearing design, cost and weight are important factors. Due to the low height of the magnets required and the ability to be produced monolithically, the up-down configuration performs the best in cost effectiveness and weight effectiveness. If the cost and weight are of less importance the left-right magnetization configuration is the better choice.

The model is validated for use with the APG 513 A ferrofluid. The EFH3 fluid shows effects that can be linked to accumulation of particles at the magnet surface. Using the APG 513 A ferrofluid a load capacity of 1.75e4 N/m^2 was achieved. Potentially this can be higher when the bearing pad is combined with a ferrofluid with a high saturated magnetization and a high colloidal stability in order to prevent accumulation.

The bearing pad that is created using the design guidelines developed in this paper can be used instead of single seal pressure bearing pads without a loss in load capacity, but with an improvement in the repeatability in fly height. Although some precision systems require more load capacity and stiffness, the achieved performance will satisfy the demands in many applications.

The novel contribution of this paper is an understanding of the influence of the parameters in the design of a pressure bearing pad and its performance in relation to the pocket bearing. This ferrofluid bearing pad is a cost-effective passive bearing alternative in motion systems in which otherwise active bearings would have been used in order to prevent all risks of stick-slip.

Author contribution

Stefan W.M. van den Toorn: Researcher; Jo W. Spronck: Supervisor; Ron A.J. van Ostayen: Supervisor; Stefan G.E. Lampaert: Supervisor

Declaration of competing interest

None.

References

[1] Ming Qiu, Long Chen, Yingchun Li, Jiafei Yan, Bearing Tribology: Principles and Applications, Springer, 2017.
[2] B. Armstrong, Stick slip and control in low-speed motion, IEEE Trans. Automat. Contr. 38 (10) (1993) 1483–1495.
[3] Wardle Frank, Ultra Precision Bearings, vol. 2, Elsevier Ltd, 2015.
[4] S.G.E. Lampaert, J.W. Spronck, R.A.J. van Ostayen, Load and stiffness of a planar ferrofluid pocket bearing, Proc. IME J. J. Eng. Tribol. 232 (1) (2018) 14–25.
[5] S Papell Solomon, Papell - 1965 - Low Viscosity Magnetic Fluids Obtained by the Colloidal Suspension of Magnetic Particles, US patent, 1965.
[6] R. Rosensweig, Buoyancy and Stable Levitation of a Magnetic Body Immersed in a Magnetizable Fluid, 1966.
[7] E. Ronald, Rosensweig. *Ferrohydrodynamics*, Dover Publications, 2013.
[8] S. van Veen, Planar Ferrofluid Bearings, MSc Thesis, 2013.
[9] Joe S. Hunter, Little J. Little, Magnetic Fluid Bearing Accelerometer, 2010.
[10] B. Assadsangabi, M.H. Tee, K. Takahata, Ferrofluid-assisted levitation mechanism for micromotor applications. *2013 Transducers and eurosensors XXVII: the 17th international Conference on solid-state sensors*, Actuators and Microsystems, TRANSDUCERS and EUROSENSORS 2013 17 (June) (2013) 2720–2723.
[11] G. Millet, Arnaud Hubert, Design of a 3 DOF Displacement Stage Based on Ferrofluids, Actuators'06, 2006, pp. 656–659.
[12] A.S.T. Boots, L.E. Krijgsman, B.J.M. de Ruiter, S.G.E. Lampaert, J.W. Spronck, Increasing the load capacity of planar ferrofluid bearings by the addition of ferromagnetic material, Tribol. Int. 129 (May 2018) (2019) 46–54.
[13] A.B. Comsol, COMSOL Multiphysics 5 (2019), 4.
[14] The Mathworks Inc. Matlab R2018b, 2018.
[15] Z.Q. Zhu, D. Howe, Halbach permanent magnet machines and applications: a review, IEE Proc. Elec. Power Appl. 148 (7) (2001) 299–308.
[16] HKCM.de. HKCM Engineering e.K. Online magnet design.
[17] Larry W. Fullerton, Mark D. Roberts, Magnetizing Printer and Method for Re-magnetizing a Least a Portion of a Previous Magnetized Magnet, 2016.
[18] Larry W. Fullerton, Mark D. Roberts, Jason N. Morgan, System and Method for Producting Magnetic Structures, 2019.
[19] H. Meng, J.N. Morgan, Q.F. Wei, C.H. Chen, Design of smart magnetic devices, in: Proceedings of 25th International Workshop on Rare-Earth and Future Permanent Magnets and Their Applications, 2018.
[20] e.K. Hkcm Engineering, Magnet-Cuboid Q50x02x02Ni-N35, 2019.
[21] S. Odenbach, Recent progress in magnetic fluid research, J. Phys. Condens. Matter 16 (32) (2004).
[22] Ferrotec, Data Sheet APG 2100 Series, 2013.
[23] J.M. Guldbakke, J. Hesselbach, Development of bearings and a damper based on magnetically controllable fluids, J. Phys. Condens. Matter 18 (38) (2006).
[24] E. Uhlmann, N. Bayat, High precision positioning with ferrofluids as an active medium, CIRP Ann. - Manuf. Technol. 55 (1) (2006) 415–418.
[25] L. van Moorsel, A Planar Precision Stage Using a Single Image Sensor, MSc Thesis, 2017.
[26] R. Deng, S. Van Veen, M. Café, J.W. Spronck, R.H. Munnig Schmidt, Linear nano-positioning stage using ferrofluid bearings, in: Conference Proceedings - 14th International Conference of the European Society for Precision Engineering and Nanotechnology, EUSPEN 2014, vol. 1, 2014, pp. 372–375. June.
[27] Max Café, Spronck Jo, Nanometer precision six degree s of freedom planar motion stage with ferrofluid bearings, in: DSPE Conference on Precision Mechatronics, 2014, pp. 43–46.